A MODIFIED MODEL FOR VISUAL DETECTION*

DR. ROBERT C. SUGARMAN, Research Psychologist
AND
MESSRS. HARRY B. HAMMILL, Research Physicist and
JEROME N. DEUTSCHMAN, Principal Engineer
Cornell Aeronautical Laboratory, Inc.

The requirement to predict the human ability to visually search and detect has occurred in a wide variety of problem areas. At Cornell Aeronautical Laboratory, Inc. (CAL) specific areas involved both ground-to-air and air-to-air search for aircraft against a sky background, and the search for small targets presented in simulator displays.

Models to predict human visual performance have been available for some time. The purpose of our paper is twofold: (1) To present a modified version of a widely known visual detection model and; (2) to compare the predictive capability of the modified version with both the original model and results of field tests involving ground-to-air search for aircraft.

THE MODEL

The first comprehensive work on visual search of a homogeneous background was done by Craik in the early 1940's. The results of his study, along with those of other studies to account for performance degradation due to atmospheric haze and to describe the detection process in a probabilistic fashion, have been organized by Koopman (1946) into a very workable and convenient model. Although the model is widely known, it is necessary to summarize its main features for this discussion:

1. In free search the eye does not scan continuously, but jumps from point to point. The eye remains fixed at each point for approximately 1/3 second for search in a homogeneous or unstructured background although longer fixation or "glimpse" times can be anticipated for search in complex backgrounds. The point in the visual field conjugate to the center of the fovea (retinal region of maximum acuity) is known as the point of fixation.
2. Target contrast (C) is defined as the average luminance difference between the target and its background, divided by the background luminance. The threshold contrast of a target (C_t) is the contrast at which the detection probability for a single glimpse assumes some nominal value. Koopman has employed a probability value of 0.57, and has expressed the threshold contrast for a single glimpse by:

$$C_t = \begin{cases} k_1 \theta^{k_2} + \dfrac{k_3 \theta^{k_4}}{\alpha_2} & (\theta \geq \theta_f) \\ k_1 \theta_f^{k_2} + \dfrac{k_3 \theta_f^{k_4}}{\alpha^2} & (\theta < \theta_f) \end{cases} \qquad (1)$$

*This work was sponsored by the United States Air Force under contract number F33615-68-C-1319.

where: θ = angle subtended at the eye (in degrees) between the point of fixation and the target ($\theta \leq 90°$)

θ_f = half-angle of fovea ($\theta_f = 0.8°$)

α = average angular diameter (minutes of arc) of the target subtended at the eye

$k_1 = 0.0175$ $\quad k_3 = 0.19$

$k_2 = 0.5$ $\quad k_4 = 1.0$

3. The probability of detection (g) during a single glimpse depends only on the ratio of target contrast to the threshold contrast of the eye (C/C_t) and is given in figure 1.

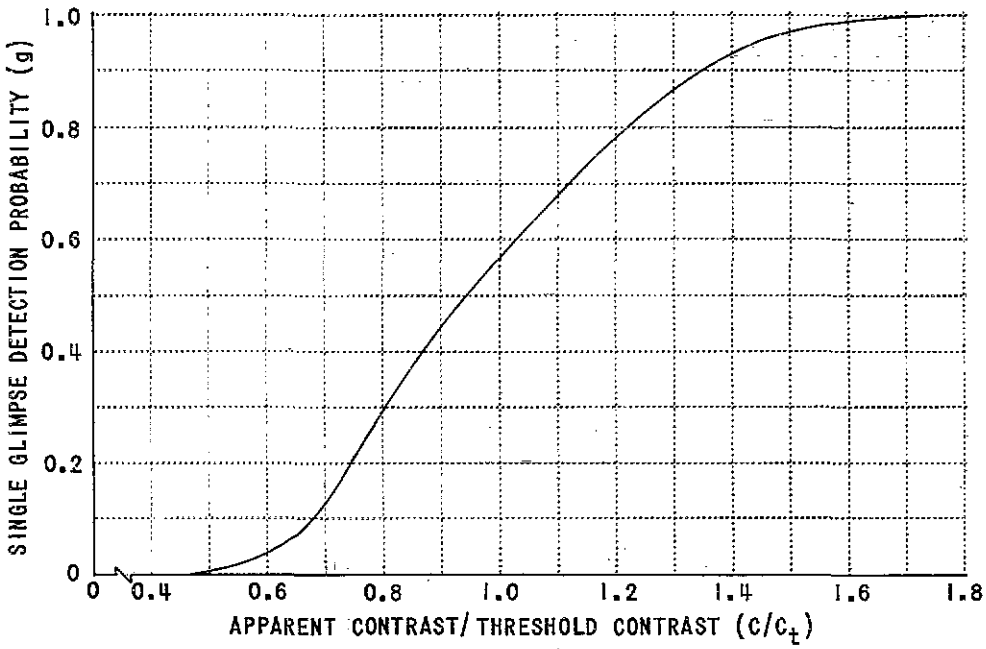

Figure 1. Glimpse Probability of Detection "g" vs Apparent Contrast/Threshold Contrast, C/C_t

4. Contrast is degraded by the atmosphere. Due to scattering by haze, the apparent target contrast (contrast seen by the observer) is reduced according to path length and haze concentration. The haze concentration is determined from the meteorological range, a mathematically precise measure designed to correlate with the general ability of the human to see through the atmosphere. The relation between the the contrast apparent to an observer (C) and the inherent contrast (C_o) was given by Middleton (1968) for horizontal view paths:

$$C = C_o e^{-\sigma R} = C_o e^{-\frac{(\ln 50)R}{V}} \qquad (2)$$

where: σ = optical attenuation coefficient of atmosphere (meters^{-1})

R = separation distance between observer and target (meters)

V = meteorological range (meters)

An account of atmospheric degradation for slant paths requires a much more complex mathematical description. Since such a generalization is peripheral to the theme of our paper, we shall confine our discussion to view paths that are essentially horizontal.

5. The search procedure consists of "continuously glimpsing" (one glimpse after another) at spatially random points within the designated search field. The probability of detecting the target during a single glimpse (instantaneous probability) is given by simply averaging "g" over the search field:

$$\bar{g} = \frac{2\pi}{M^2\Omega} \int_0^{\theta_0} g(\theta) \sin\theta \, d\theta \qquad (3)$$

where: $\bar{g}$ = average detection probability for single glimpse

Ω = solid angle of search field

θ_0 = one-half the apparent field of view of optics (e.g. 90° unaided eye, 28° binoculars)

M = linear magnification of optics

It should be noted that in addition to the search field Ω, an account of masking by the field stop is also included.

MODEL MODIFICATION

The model described above has undergone two modifications during its use at CAL. First, the mathematical expression relating threshold contrast, target size, and position in the visual field has been adjusted to agree with specific data subsequently published in the literature. The motivation for this was our feeling for some time that the detection ranges predicted by the model were on the high side.

Second, the actual distributions of the peripheral angle (angle between the aircraft and the visual fixation point subtended at the observer) have been generated for various postulated geometric configurations involving the search field, target location and random search distribution. These distributions are used as a base for computing the average glimpse detection probability $\bar{g}$. (Although only specific distributions were employed in our study, any configuration can be handled by generation of its corresponding distribution.) Prior to the use of these distributions, the integration involved in determining $\bar{g}$ assumed the significant region of the visual field was completely contained within the search field, an approximation that allowed the simple integration procedure indicated by Equation (3).

---

*For our application, Weber's Law states that the brightness difference at threshold is proportional to background brightness.

MODEL ADJUSTMENT TO NEW DATA

The threshold contrast expression (Equation (1)) was adjusted to fit threshold data published by Sloan (1961). Sloan has measured, for monocular viewing, "just perceptable differences" of small stimuli against a uniform background. She presented oval stimuli of uniform luminance for durations of approximately one second. The range in angular subtense (average diameter) at the eye was from 3 min of arc to 100 min. The "oval" nature of the stimuli resulted from optical distortion in the apparatus, not design, but the ratio of largest to smallest dimension was always less than 2:1. The thresholds were taken at a background luminance of 3.16 mL (10 nit) and include the dependence on position in the visual field. Only stimuli brighter than the background were used.

Initially there were two points of concern regarding the use of the Sloan data with the background level of 10 nit since this level is two to three orders of magnitude smaller than the daytime sky. The first relates to the validity of Weber's Law* which provides that background and stimulus brightness affect target detection only through contrast. Pirenne (1962) clearly illustrates (figure 2a) the validity of the law for retinal illumination levels above 1000 trolands. However, Sloan's background of 10 nit results (via adaptation) in an eye pupil diameter of 4 mm (LeGrand - 1957) thus yielding a retinal illumination of only 125 trolands. It is seen from figure 2a that the departure from Weber's Law is very small at this level and one can anticipate that the error arising from the departure may be negligible compared to the correction obtained by employing the Sloan data.

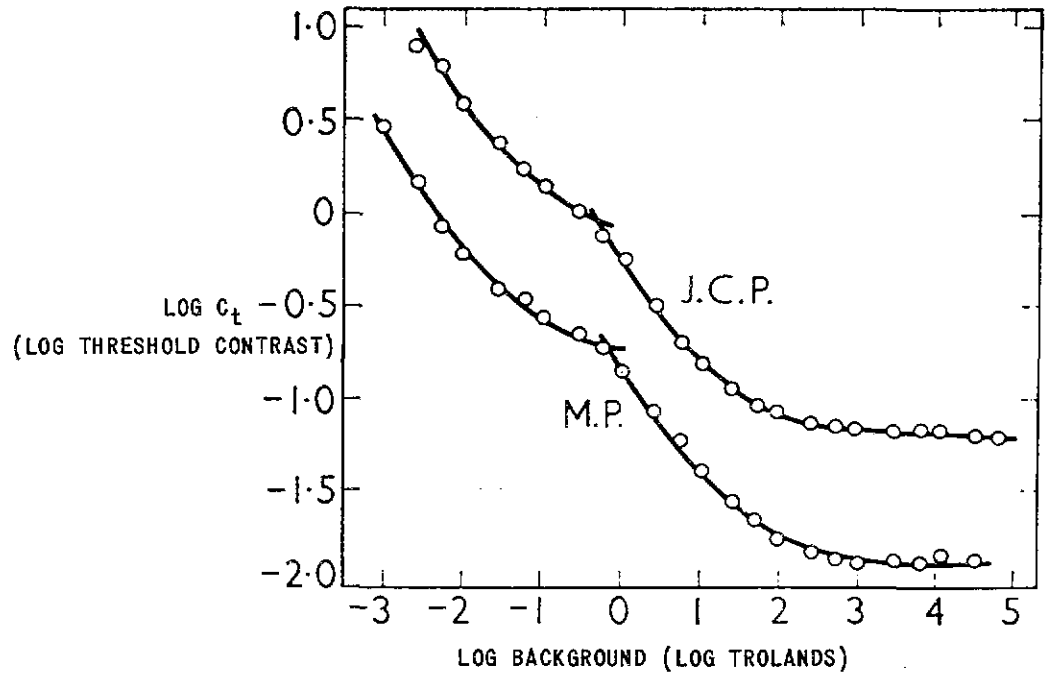

a. Threshold Dependence on Background for Two Observers (J.C.P., M.P.) (The Points for M.P. have been lowered 0.5 Log Units)

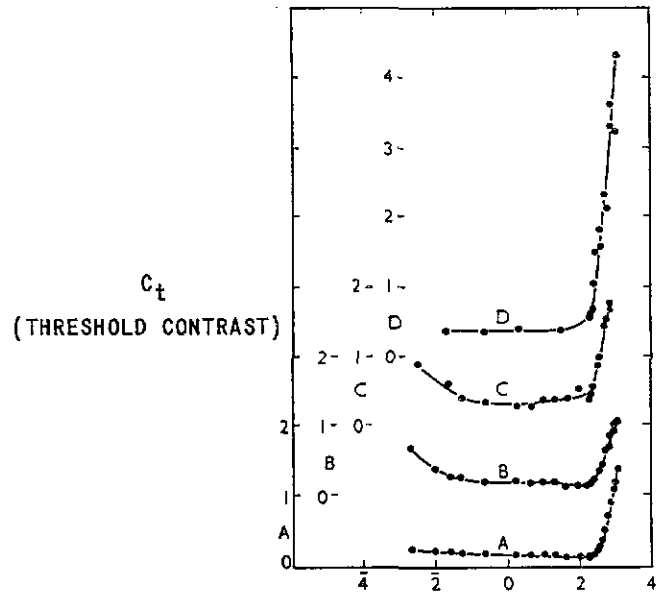

b. Threshold Dependence of Rods Only on Background For 4 Observers (A,B,C,D)

Figure 2. Threshold Dependence on Background Luminance (After Pirenne - 1962) (Reproduced through permission of Copyright Holder, Academic Press, 1962)

The second point of concern was regarding the role of the rods in the detection process. The spectral distribution of Sloan's background and stimulus was essentially that of Illuminent A (Tungsten) and therefore the illuminance of 125 trolands converts to 70 scotopic trolands when adjusting for the spectral response between cones and rods. It is seen (figure 2b) that this falls in the upper part of a sensitivity range for which Weber's Law is valid for the rods. Also it is a range of maximum contrast sensitivity (minimum contrast threshold) of the rods which does not correspond at all to sky background at which rod saturation is achieved. Although this difference exists, it is not believed to be important since, as indicated in figure (2a), the transition from cones to rods as the determinant of threshold occurs slightly below 1 troland and Sloan's value of 125 trolands provides a safety factor of two orders of magnitude.

There are three points that should be made regarding Equation (1). The first relates to the rotational symmetry of C_t about the fixation point. Equation (1) provides that C_t does not depend on both angular coordinates of the stimulus in the visual field, but only on the difference angle between the stimulus and the fixation point. Although Sloan's data indicate an asymmetry (primarily in the horizontal meridian) it is not large, and is somewhat averaged out for an observer using both eyes. Second, no statistical definition of threshold contrast was used by Sloan, so we assume her data to lie in the region of 50% detection probability, and therefore they were arbitrarily equated to C_t of Equation (1). Should the assumption be proved invalid the abscissa of the single glimpse probability curve (Figure (1)) can be scaled accordingly. The third point relates to the dependence of threshold contrast on stimulus size. Sloan states that the data are usually fitted by an equation of the form:

$$C_t = \beta_2 (\alpha^2)^{-\beta_1} \qquad (4)$$

where β_1 and β_2 depend only on position in the visual field. Of the two possibilities for fitting a model to Sloan's data (Equations 1 or 4) Equation (1) was used since it is more reasonable asymptotically for both small and large α. The difficulty with Equation (4) can be understood by considering the asymptotic constraints on β_1. As α becomes small, point stimuli are approached and C_t must vary as α^{-2} thereby requiring $\beta_1 = 1$. For large α, we expect C_t to be relatively insensitive to α thereby indicating a β_1 close to zero. Since β_1 does not depend on α, Equation (4) cannot hold over such a large α range, and we shall not consider it further.

The data selected for fitting Equation (1) is shown in figure (3a). This data was fitted by varying $k_1 \ldots k_4$ of Equation (1) to minimize a square error (ϵ). It was decided to minimize in log space without a weighting function. That is:

$$\epsilon = \sum_{\substack{\text{data} \\ \text{points} \\ (\theta \neq 0)}} \left(\eta_{d.p.} - \eta_{Eq.(1)}\right)^2 \tag{5}$$

where η is the log of the threshold brightness difference in units of $\log \mu L$. The value of $\eta_{Eq.(1)}$ is related to C_t of Equation (1) by:

$$\eta = \log C_t + 3.5 \tag{6}$$

The term "3.5" in Equation (6) is simply the log of Sloans background luminance in $\log \mu L$.

The square error (ϵ) of Equation (5) was minimized using a direct search procedure which resulted in the following new values:

$$\begin{aligned} k_1 &= 0.0265 & k_3 &= 0.44 \\ k_2 &= 0.24 & k_4 &= 1.6 \end{aligned} \tag{7}$$

It is the replacement of these k values for those indicated in Equation (1) that comprises the major modification of the visual detection model. Threshold curves (in the ordinate η) are shown in figures (3b) and (3c) for the former and the present values of k respectively. The new values provide a substantially better fit to the data, with the most significant change being a large increase in the threshold for small stimuli in the peripheral region.

PERIPHERAL ANGLE DISTRIBUTIONS

The determination of the single glimpse detection probability (g in figure (1)) requires specification of the threshold contrast C_t which in turn depends on the peripheral angle (θ) in Equation (1). That is, formal elimination of C_t between Equation (1) and figure (1) allows us to write:

$$g = g(\theta) \tag{8}$$

where the arguments C and α have been dropped since our interest here is only with the angle θ. The peripheral angle θ is the angular difference (at any instant) between the stimulus (target) and the visual fixation point subtended at the observers eye. Since it is customary to treat the target and fixation

positions as random variables, the peripheral angle is also a random variable. Thus in order to establish an explicit value of detection probability at any "instant" (single glimpse), it is necessary to specify the target and fixation positions as probability distributions, and compute an expected value ($\bar{g}$) over the search field.

The original model assumes a uniform distribution of target position within the search field. It was further assumed that the region of the visual field surrounding the fixation which is important to detectability in the practical case is small, and therefore the border of the search field can be ignored when carrying out the averaging integral. These two assumptions allow $\bar{g}$ to be written according to Equation (3).

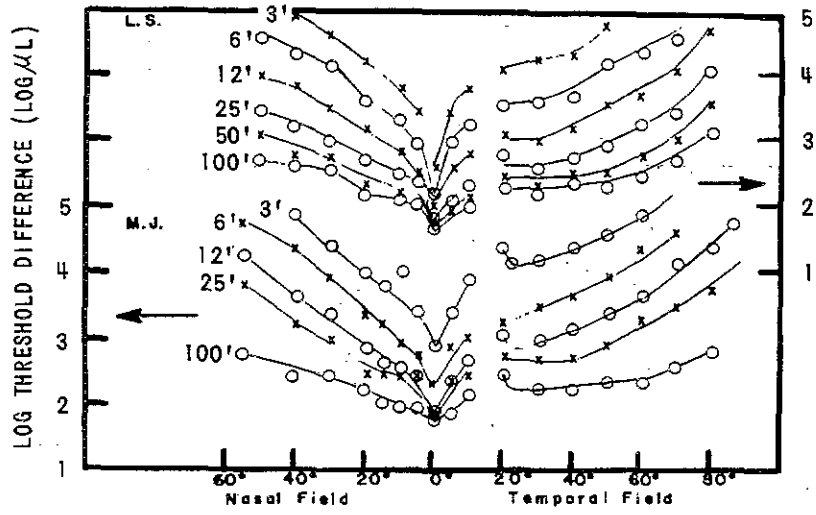

a. Threshold Gradients in the Horizontal Meridian
The Size of the Test Object is Shown at the left
Of Each Curve (After Sloan - 1961)

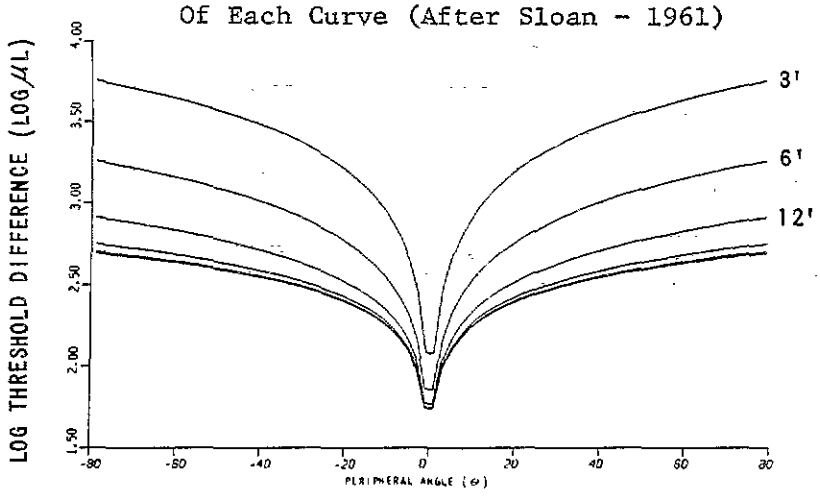

b. Threshold Gradients Predicted by Original Model

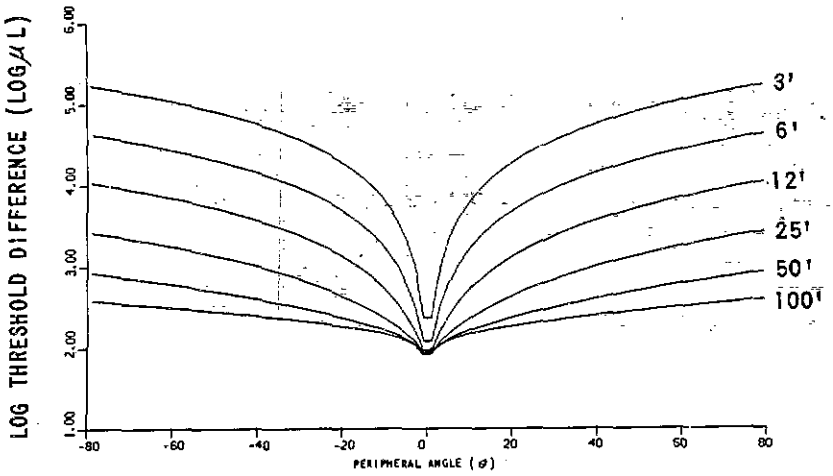

c. Threshold Gradients Predicted by Modified Model

Figure 3. Comparison of Data and Model Threshold Gradients

With regard to the two assumptions underlying Equation (3), the latter, involving negligible interaction between the visual field and search field border, is easily dropped. With complete generality we can write:

$$\bar{g} = \int_0^{\pi/2} P_e(\theta)\, g(\theta)\, d\theta \tag{9}$$

Where $P_e(\theta)$ is the actual probability density of the peripheral angle θ and includes all the information defining the search field, optical magnification and the distributions of target and fixation within the search field. The establishment of distributions (P_e) for the search configurations of interest and the computation of $\bar{g}$ through Equation (9) are, in essence, incorporated in the present model as a replacement for Equation (3).

The use of the distribution $P_e(\theta)$ is somewhat clumsy due to the dependence on optical magnification. That is, a separate distribution would have to be generated for each magnification value desired in order to compute $\bar{g}$. It was found to be convenient to write Equation (9) in terms of the angle (θ') separating the target and corresponding fixation point as it occurs in the actual search field Ω_o. Clearly, the relation between θ and θ' is:

$$\theta = M\theta' \tag{10}$$

Where: θ = peripheral angle within visual field (at eye)

θ' = peripheral angle in real world.

In terms of θ', Equation (9) can be written*:

$$\bar{g} = \int_0^{\pi} P(\theta')\, g(M\theta')\, d\theta' \tag{11}$$

*The Upper limit of π in Equation (11) is symbolic. It simply implies the integration is carried out until either P or g becomes zero. It was used to provide validity should the magnification ever be less than unity.

Where $P(\theta')$ is the probability density of the angle θ', and is independent of magnification.

Initially it was attempted to generate $P(\theta')$ distributions assuming the target and fixation distribution were distributed uniformly within the search field and a corresponding equation for the distribution is derived in the appendix. This approach was abandoned since it was too time consuming on the computer. It was decided instead to compute $P(\theta')$ for specific target positions, and the equation for this distribution is also given in the appendix.

Specific distributions were generated again assuming a uniform fixation density within various search fields of interest, and examples of the distribution are shown in figure (4). The fine structure along the tops of these distributions is coherent noise in the form of a moiré pattern resulting from overlapping of the search field border and the discretely sampled coordinate system used in the actual computer calculation of the distributions. The fluctuations are small and can be ignored.

The distributions were punched on cards and are available as data arrays within the computer verison of the present model. Computer test runs indicate only slight differences between the detection probability values resulting from the former and present expressions for $\bar{g}$ (Equations (3) and (11) for the search geometries of interest in the present study. However, other search configurations may result in large differences and for that reason, Equation (11) should be employed.

COMPARISONS OF ORIGINAL MODEL, MODIFIED MODEL, AND FIELD TEST RESULTS

Having made the two model modifications just discussed, the next step was to determine the present model's predictive capability by comparison of the original and modified detection models with experimental results reported in the literature. An attempt at such comparisons quickly revealed the difficulties that are encountered when trying to verify a model with experimental data obtained from tests not designed specifically for verification of the particular model. Usually the experimental data are incomplete in their specification of one or more of the conditions of the experiment which are necessary for model inputs, i.e., contrast, meteorological range, glimpse time, target area, and search field size.

One notable exception is the experimental work reported by E.K. Seyb (1966) in which results are given for detections by the unaided eye from field tests conducted in Germany. The results are plotted in a meteorological visibility-detection range coordinate system, with cumulative probability of detection as a parameter, for the typical parameter values given in table 1. Seyb also mentions that, "as far as meteorological visibility was concerned, the test results of the German field tests were only available in intervals of 2 km." The experimental data were converted for purposes of the present study, to cumulative probability of detection versus range for constant values of meteorological visibility. This form of the data is compared with results obtained from runs of both the original and modified models using as inputs the values given in table 1.

It should be noted that the only reference to aircraft size is through the visible area of 5.5 meters^2. The aircraft was not specified by Seyb, but since the altitude is low, and radial flight paths were employed, the visible area was not varied during the computer runs.

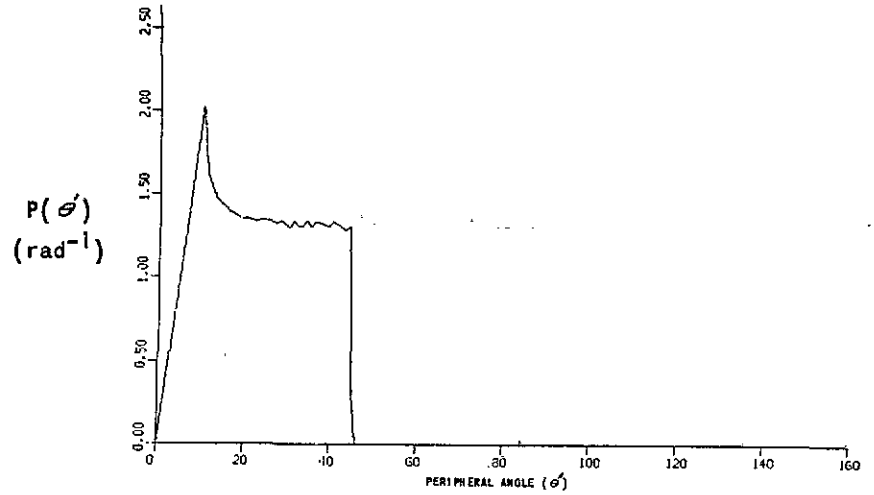

a. Target Centered within Search Field

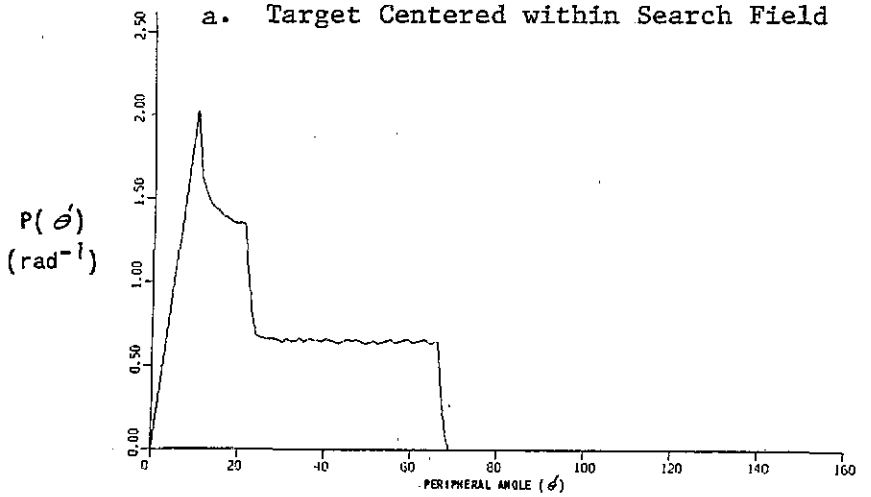

b. Target Horizontally Offset 23° From Center

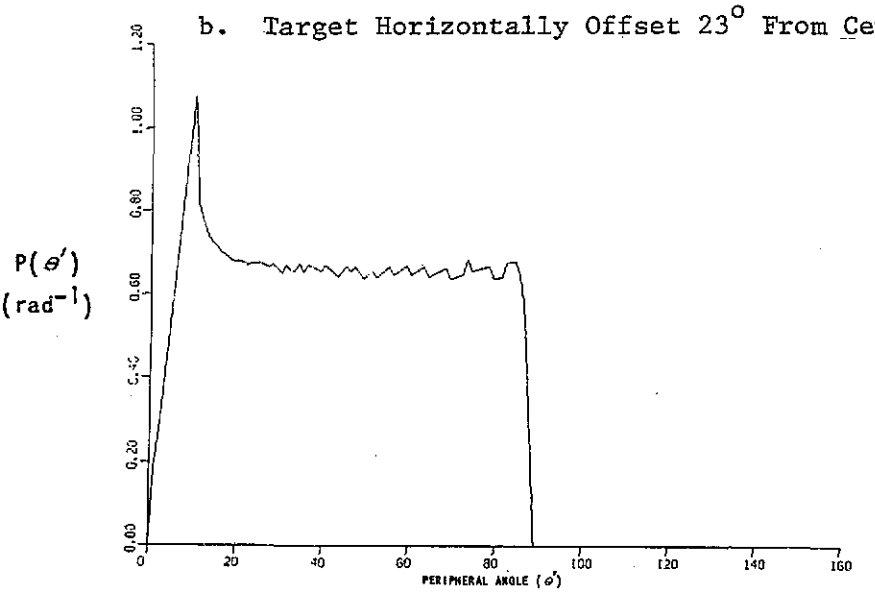

c. Target Horizontally Offset to Edge of Search Field

Figure 4. Peripheral Angle Distributions for a Search Field 90° in Azimuth and to 20° Above the Horizon

TABLE 1. FIELD TEST CONDITIONS
(AFTER SEYB - 1966)

Parameters	Mean Values
Velocity	60 m/s
Altitude	0.1 km
Offset	0.0 km
Inherent contrast, C_o	0.93
Glimpse Time	1.5 sec
Visible area	5.5 m^2
Search Field Size	30° Az x 5° El
Meteorological Range	5, 7, 17, 21 km

We should also mention that it was necessary to assume a target position within the 30° x 5° search field in order to generate a peripheral angle distribution for the modified version of the model. A location of 5° Az from the search field center, and 2° El above the horizon was employed.

Figures 5a and 5b compare experimental results with model prediction for meteorological visibilities of 21 and 17 km, respectively. Experimental data points are represented by circles. The theoretical predictions include those made using the original model as well as those obtained using the modified model. It is readily seen that for a given probability of detection, the original model results consistently predict greater ranges of detection than the modified model. Additionally, the modified model predicts the experimental data fairly well. Results for meteorological visibilities of 7 and 5 km are shown in figures 6a and 6b, respectively. Here, again it may be seen that the cumulative curves obtained with the original model lie at greater ranges than those obtained for the modified model. The modified model results, again, lie closer to the experimental data. The larger discrepancy between model and experimental results for the lower meteorological visibilities may be partially a result of the interval of presentation of the data; i.e., test results were available only in intervals of 2 km.

SUMMARY

The primary result of this study has been the modification of an existing visual detection model to provide better agreement with known performance data. Comparisons with field data have shown the modified version to be preferable to the original, since the original predicts a highly optimistic detection performance. Based on these comparisons, we recommend the use of the modified version in problem areas whose conditions are consistent with the model features described above.

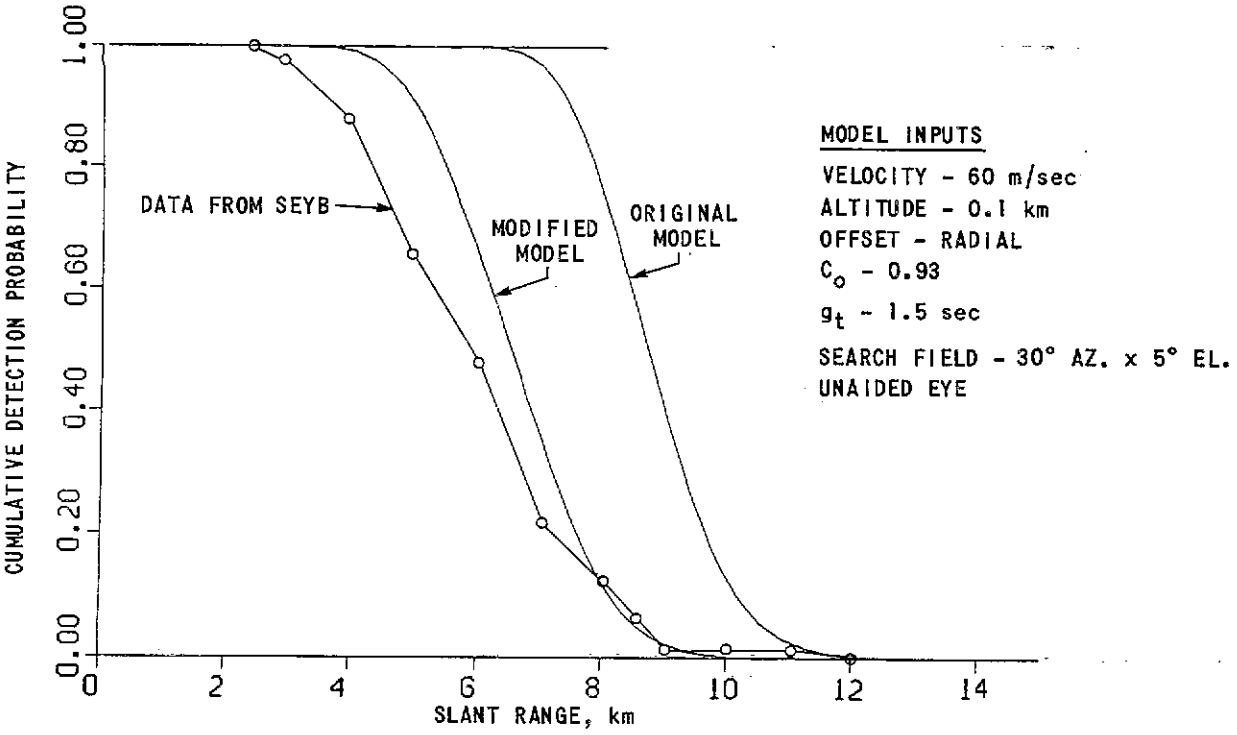

Figure 5a. Cumulative Detection Probability-Comparison of Model Results and Field Data with 21 KM Visibility

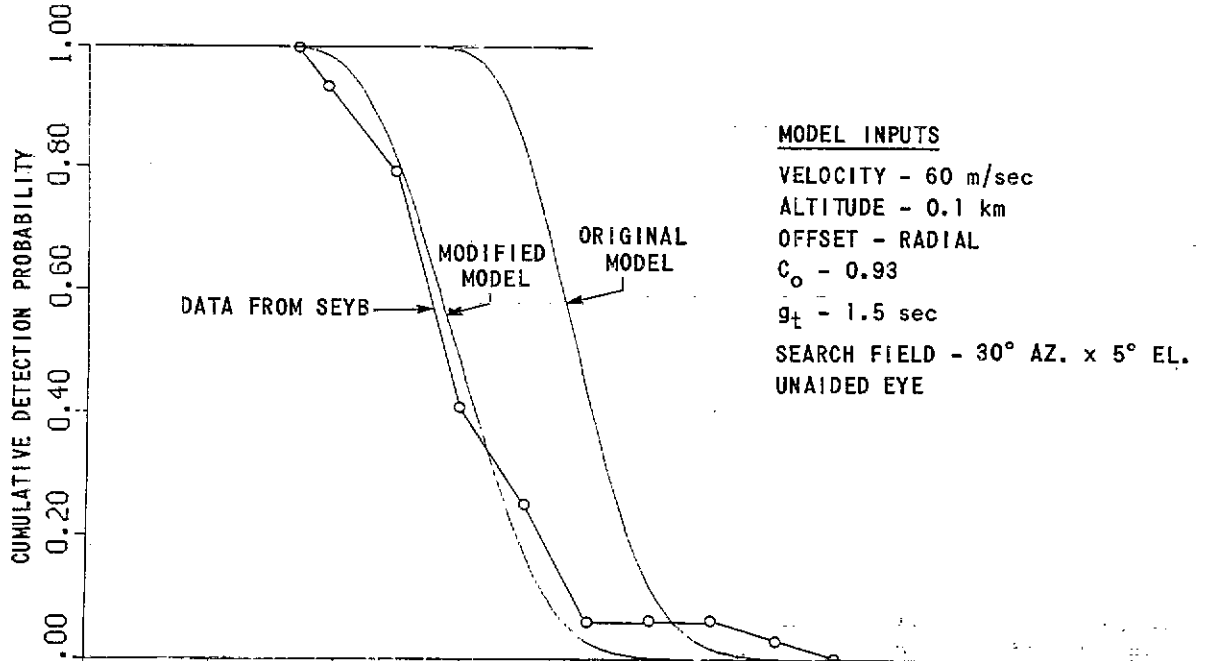

Figure 5b. Cumulative Detection Probability-Comparison of Model Results and Field Data with 17 KM Visibility

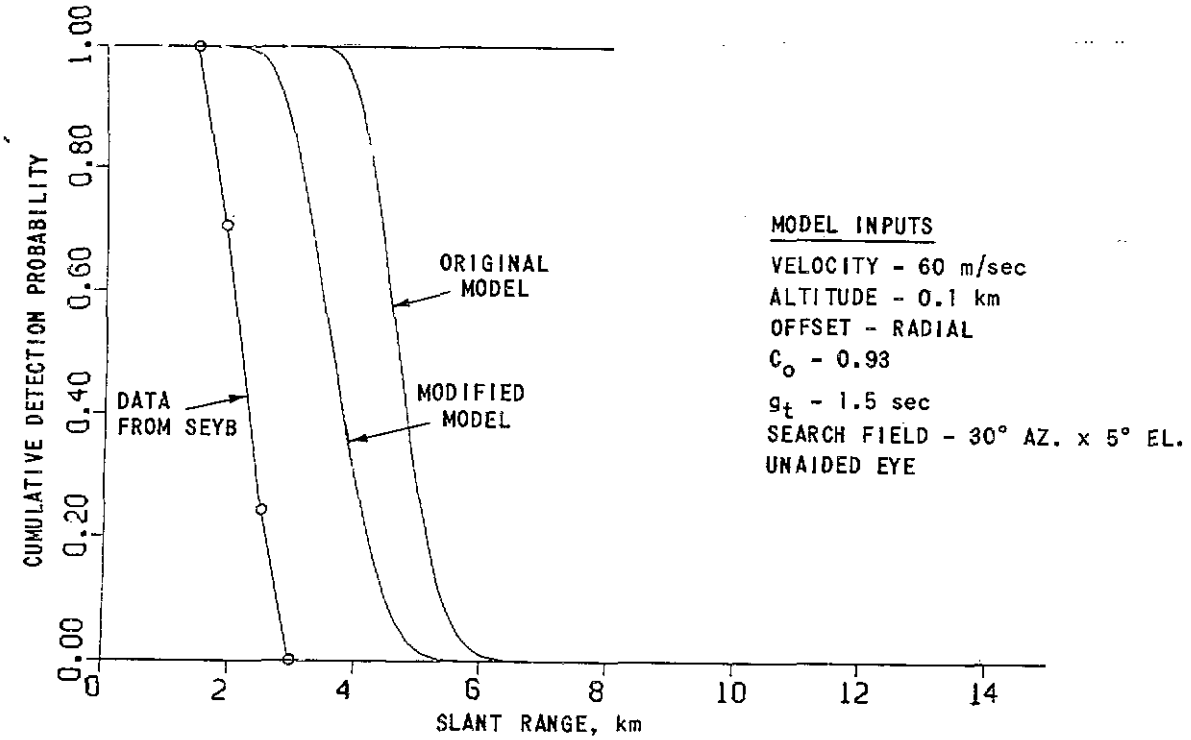

Figure 6a. Cumulative Detection Probability-Comparisons of Model Results and Field Data with 7 KM Visibility

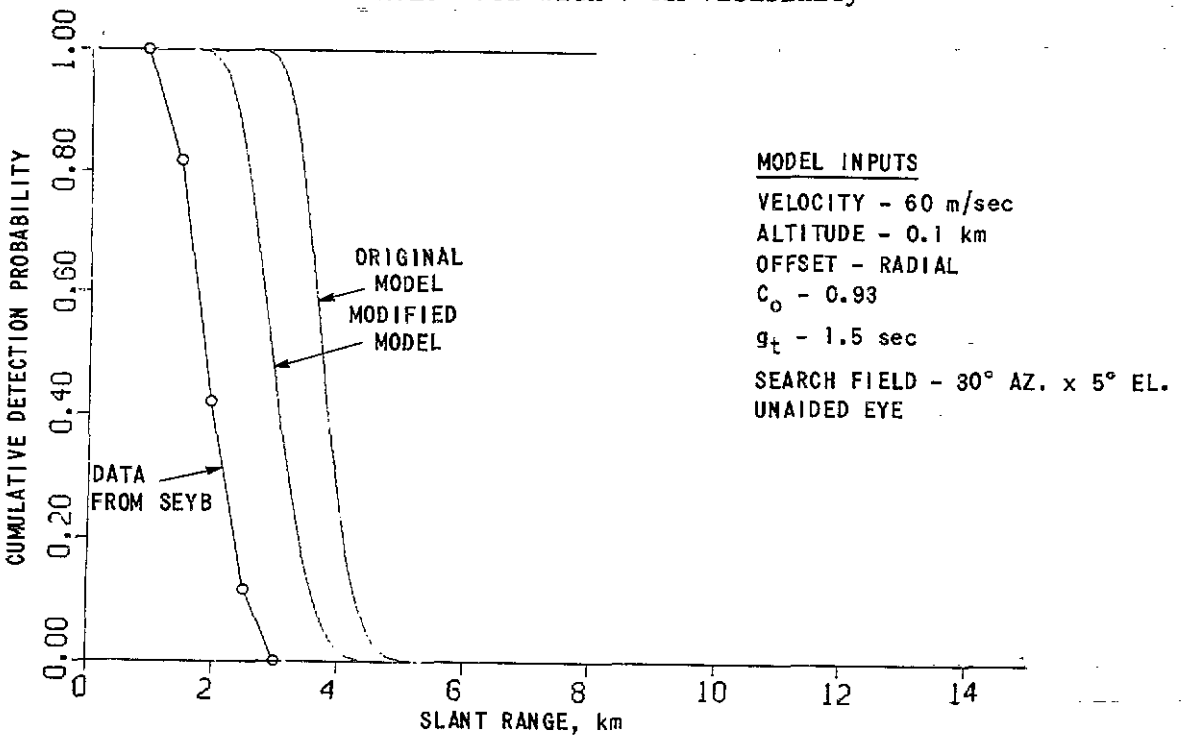

Figure 6b. Cumulative Detection Probability-Comparison of Model Results and Field Data with 5 KM Visibility

References

B.O. Koopman, "Search and Screening," Navy, Operations Elevation Group Report No. 56 (1946).

Y. LeGrand, "Light Colour and Vision," Chapman and Hall (1957).

W.E.K. Middleton, "Vision Through the Atmosphere," Univ. of Toronto Press (1968).

M.H. Pirenne, "Liminal Brightness Increments," Contained in H. Davson (editor), Volume 2 "The Eye," Academic Press (1962).

E.K. Seyb, "A Study on Ground-to-Air Visual Detection," SHAPE Technical Center, Professional Paper PP-4 (December 1966).

L.L. Sloan, "Area and Luminance of Test Object as Variables in Examination of the Visual Field by Projection Perimetry," Vision Research 1, 1/2 p. 121 (June 1961).

APPENDIX A

The single glimpse detection probability ($\bar{g}$) is obtained by use of the relation:

$$\bar{g} = \int_0^{\pi} P(\phi_2'')\, g(M\phi_2'')\, d\phi_2'' \qquad \text{(A-1)}$$

where:

ϕ_2'' = real difference angle between target position and fixation point*

$g(M\phi_2'')$ = single glimpse detection probability

$P(\phi_2'')$ = probability density of ϕ_2''

M = magnification of optics ($M = 1$ for unaided search)

This appendix shows the procedure for generating the $P(\phi_2'')$ distributions as they depend on the independent distributions of target position and fixation point within a search field Ω_0. The situation is most easily understood by examining figure A-1. The two vectors representing target and fixation direction are unit vectors. All angles subscripted "1" are target coordinates, and "2" are fixation coordinates. The fixed frame x, y, z is that of the search field Ω_0.

*The difference angle ϕ_2'' is the same as θ' in the main text. As a matter of convenience, the notation used in this appendix and the main text were not forced to agree.

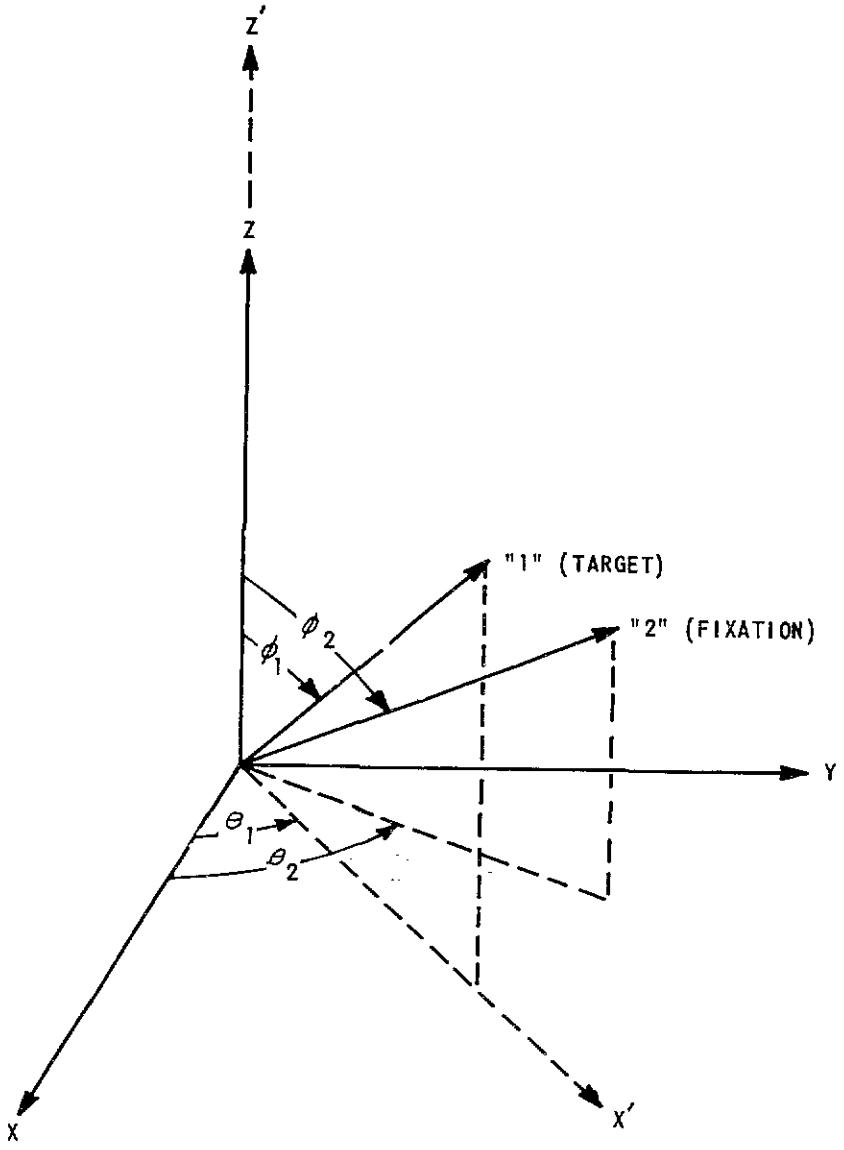

Figure A-1. Geometry of Target and Fixation Vectors

The distribution $P(\phi_2'')$ is found by integrating over the joint probability distribution of the two vectors. For a target vector within $d\Omega_1$, and a fixation vector within $d\Omega_2$, the joint probability can be written:

$$dP = P_1(\theta_1, \phi_1)\, P_2(\theta_2, \phi_2)\, d\Omega_1\, d\Omega_2 \qquad \text{(A-2)}$$

$$= P_1(\theta_1, \phi_1)\, P_2(\theta_2, \phi_2)\, \sin\phi_1 \sin\phi_2\, d\theta_1\, d\phi_1\, d\theta_2\, d\phi_2$$

where P_1 , and P_2 are the distributions of the target and fixation respectively.

We wish to integrate out three coordinates in such a way as to leave only the coordinate ϕ_2''. Since ϕ_2'' is not among the four coordinates of Equation A-2, it is first necessary to transform coordinates.

The transformation consists of a coordinate rotation to provide that the new z direction will coincide with the target vector, thus establishing that the new ϕ coordinate of the fixation will be the desired difference angle. The transformation is carried out in two steps. First is a rotation about the z axis through the angle θ_1 to place the target vector in a new x', z' plane:

$$\begin{pmatrix} x' \\ y' \end{pmatrix} = \begin{pmatrix} \cos\theta_1 & \sin\theta_1 \\ -\sin\theta_1 & \cos\theta_1 \end{pmatrix} \begin{pmatrix} x \\ y \end{pmatrix} \; ; \quad z' = z \tag{A-3}$$

Second is a rotation about the y' axis through the angle ϕ_1, to finally put the target vector in the new z'' direction:

$$\begin{pmatrix} x'' \\ z'' \end{pmatrix} = \begin{pmatrix} \cos\phi_1 & -\sin\phi_1 \\ \sin\phi_1 & \cos\phi_1 \end{pmatrix} \begin{pmatrix} x' \\ z' \end{pmatrix} \; ; \quad y'' = y' \tag{A-4}$$

Since ϕ_2'' is the desired difference angle, we formally replace θ_2, ϕ_2 with θ_2'', ϕ_2''. Equation (1) thus becomes:

$$dP = P_1(\theta_1, \phi_1)\, P_2(\theta_2, \phi_2)\, \sin\phi_1 \sin\phi_2''\, d\theta_1\, d\phi_1\, d\theta_2''\, d\phi_2'' \tag{A-5}$$

Integrating over θ_1, ϕ_1 and θ_2'' yields the density $P(\phi_2'')$:

$$P(\phi_2'') = \sin\phi_2'' \int \sin\phi_1 \left\{ \int P_1(\theta_1, \phi_1) \left[\int P_2(\theta_2, \phi_2)\, d\theta_2'' \right] d\theta_1 \right\} d\phi_1 \tag{A-6}$$

where the integrals are taken over all space.* Before the inner integral can be performed, it is necessary to establish the relation between the old and new coordinates. That is, Equation (A-6) specifies θ_2'', ϕ_2'' and it is necessary to know θ_2, ϕ_2 in order to evaluate P_2. The components of the target vector in both systems are written:

$$\left.\begin{aligned} x'' &= \sin\phi_2'' \cos\theta_2'' & x &= \sin\phi_2 \cos\theta_2 \\ y'' &= \sin\phi_2'' \sin\theta_2'' & y &= \sin\phi_2 \sin\theta_2 \\ z'' &= \cos\phi_2'' & z &= \cos\phi_2 \end{aligned}\right\} \tag{A-7}$$

*The information regarding the search field (Ω_o) is formally included in the distributions P_1 and P_2.

Elimination of all the components between Equations (A-3), (A-4), and (A-7) gives:

$$\begin{pmatrix} \sin\phi_2 \cos\theta_2 \\ \sin\phi_2 \sin\theta_2 \\ \cos\phi_2 \end{pmatrix} = \begin{pmatrix} \cos\theta_1 & -\sin\theta_1 & 0 \\ \sin\theta_1 & \cos\theta_1 & 0 \\ 0 & 0 & 1 \end{pmatrix} \begin{pmatrix} \cos\phi_1 & 0 & \sin\phi_1 \\ 0 & 1 & 0 \\ -\sin\phi_1 & 0 & \cos\phi_1 \end{pmatrix} \begin{pmatrix} \sin\phi_2'' \cos\theta_2'' \\ \sin\phi_2'' \sin\theta_2'' \\ \cos\phi_2'' \end{pmatrix} \quad \text{(A-8)}$$

or

$$\left.\begin{aligned} \sin\phi_2 \cos\theta_2 &= \cos\theta_1 \cos\phi_1 \sin\phi_2'' \cos\theta_2'' - \sin\theta_1 \sin\phi_2'' \sin\theta_2'' + \cos\theta_1 \sin\phi_1 \cos\phi_2'' \\ \sin\phi_2 \sin\theta_2 &= \sin\theta_1 \cos\phi_1 \sin\phi_2'' \cos\theta_2'' + \cos\theta_1 \sin\phi_2'' \sin\theta_2'' + \sin\theta_1 \sin\phi_1 \cos\phi_2'' \\ \cos\phi_2 &= -\sin\phi_1 \sin\phi_2'' \cos\theta_2'' + \cos\phi_1 \cos\phi_2'' \end{aligned}\right\} \quad \text{(A-9)}$$

The evaluation of $P(\phi_2'')$ in Equation (A-6) can now be carried out once the distributions (P_1 and P_2) are chosen.

It was attempted initially to assign uniform distributions to both P_1 and P_2 within the search field Ω_o and zero outside:

$$P_1 = P_2 = \begin{cases} 1/\Omega_o & (\text{inside } \Omega_o) \\ 0 & (\text{otherwise}) \end{cases} \quad \text{(A-10)}$$

Unfortunately, the evaluation of $P(\phi_2'')$ proved to be much too time consuming on the computer and the choice of Equation (A-10) was abandoned.

As an alternative it was decided to specify the target location within the search field thereby eliminating two of the three integrations in Equation (A-6). Formally, we write:

$$P_1(\theta_1, \phi_1) = \delta(\theta_1 - \theta_T, \phi_1 - \phi_T) \quad \text{(A-11)}$$

where δ is the Dirac delta function and θ_T, ϕ_T are the target coordinates. Equation (A-6) thus becomes:

$$P(\phi_2'') = \sin\phi_2'' \int P_2(\theta_2, \phi_2)\, d\theta_2'' \quad \text{(A-12)}$$

The reader should not be misled by the seeming absence of the target coordinates from Equation (A12) since they do enter into the required transformation of Equation (A-9).